

Multiple dielectric transitions in the $\text{PbTiO}_3\text{-Bi}(\text{Zn}_{1/2}\text{Ti}_{1/2})\text{O}_3\text{-Bi}(\text{Mg}_{1/2}\text{Ti}_{1/2})\text{O}_3$ system

David M. Stein,¹ Ilya Grinberg,² Andrew M. Rappe,² and Peter K. Davies^{1,a)}¹*Department of Materials Science and Engineering, University of Pennsylvania, 3231 Walnut Street, Philadelphia, Pennsylvania 19104, USA*²*Makineni Theoretical Laboratories, Department of Chemistry, University of Pennsylvania, Philadelphia, Pennsylvania 19104, USA*

(Received 29 December 2010; accepted 28 August 2011; published online 11 October 2011)

The ternary perovskite system $\text{PbTiO}_3\text{-Bi}(\text{Zn}_{1/2}\text{Ti}_{1/2})\text{O}_3\text{-Bi}(\text{Mg}_{1/2}\text{Ti}_{1/2})\text{O}_3$ was investigated in an attempt to capture the enhanced tetragonality of the $\text{PbTiO}_3\text{-Bi}(\text{Zn}_{1/2}\text{Ti}_{1/2})\text{O}_3$ binary system at a morphotropic phase boundary (MPB) to improve piezoelectric performance. Results from the $(1-x)[0.75\text{PbTiO}_3\text{-}0.25\text{Bi}(\text{Zn}_{1/2}\text{Ti}_{1/2})\text{O}_3]\text{-}(x)\text{Bi}(\text{Mg}_{1/2}\text{Ti}_{1/2})\text{O}_3$ pseudo-binary solution indicate the formation of an MPB-type phase boundary with a high T_C (585°C at $x = 0.55$). Multiple dielectric transitions were observed in a region of the ternary diagram characterized by high occupancy of the A-site by Bi^{3+} ($>40\%$) and the B-site by ferroelectrically active cations ($>70\%$). Temperature-dependent diffraction studies revealed the persistence of a tetragonal structure in at least a subset of the crystal to the higher temperature dielectric transition. © 2011 American Institute of Physics. [doi:10.1063/1.3646559]

I. INTRODUCTION

Bismuth has been intensely investigated as a replacement for lead in piezoelectric perovskite systems. The Bi^{3+} cation possesses the $6s$ electron pair responsible for the large displacements of Pb^{2+} in piezoelectric systems such as $\text{Pb}(\text{Zr,Ti})\text{O}_3$ and lacks the environmental and health concerns of lead.¹ Furthermore, theoretical and experimental work has shown that A-site displacements and polarization magnitudes can be significantly larger in Bi-based perovskite systems than in their Pb-based counterparts.^{2–5} Despite this, most Bi-based additives to PbTiO_3 (PT) behave similarly to PbZrO_3 . With increasing substitution, the tetragonality of the structure decreases until a morphotropic phase boundary (MPB) is formed. MPBs are crucial for piezoelectric applications, as the energy necessary to reorient the macroscopic polarization is drastically reduced relative to nearby compositions in a solid solution.

Compared to their Pb-based counterparts, Bi-based substitutions in PT can induce higher transition temperatures at the MPB (e.g., $T_C = 425^\circ\text{C}$ for $0.37\text{PT}\text{-}0.63\text{Bi}(\text{Mg}_{1/2}\text{Ti}_{1/2})\text{O}_3$ (BMT), 450°C for $0.64\text{PT}\text{-}0.36\text{BiScO}_3$). However, the larger displacements of Bi^{3+} do not enhance the macroscopic polarizations of PT.^{6,7} Correlated displacements are possible when the B-site contains a high fraction of ferroelectrically active cations capable of cooperatively displacing to minimize repulsive forces between the A- and B-sublattice.^{8,9} Consequently, additives such as $\text{Bi}(\text{Zn}_{1/2}\text{Ti}_{1/2})\text{O}_3$ (BZT) and $\text{Bi}(\text{Zn}_{3/4}\text{W}_{1/4})\text{O}_3$ (among others) allow for the correlation of individual cation displacements when added to PT by combining Bi^{3+} with known ferroelectrically active (FE-active) B-site cations.^{10–13} The $(1-x)\text{PT}\text{-}(x)\text{BZT}$ solid solution has solubility up to $x = 0.4$ with a c/a ratio of 1.11 and a T_C that

exceeds 700°C at that composition. In contrast to most additives, for these materials increasing substitution into PT increases the tetragonality of the structure until the solubility limit is reached. Increased polarization and Curie temperature (T_C) accompany the increases in tetragonality. The next step toward using these tetragonality enhancing additives in piezoelectric applications is to attempt to capture the enhanced polarization at an MPB to improve the piezoelectric response and to raise the ferroelectric to paraelectric transition temperature. To this end, we investigated the ternary system consisting of PT, the tetragonality enhancing additive BZT, and the Bi-based MPB-forming additive BMT.

II. EXPERIMENTAL PROCEDURES

Samples in the PT-BZT-BMT ternary system were prepared by traditional solid state methods from the component oxides. Stoichiometric mixtures of the starting reagents were ball milled in ethanol with yttria-stabilized zirconia balls for 5 h. To achieve phase homogeneity the powders were calcined multiple times between 850 and 1100°C . After calcination the powders were isostatically pressed into pellets, surrounded by sacrificial powder of the same composition to avoid any loss of the more volatile components, and sintered for 5 h between 1000 and 1100°C depending on the composition. Powder x-ray diffraction (XRD) patterns of calcined powders were recorded in the 2θ scan range of $15^\circ\text{--}60^\circ$; lattice parameters were calculated via the least-squares method. Neutron powder diffraction (NPD) data was collected using the BT-1 32-detector neutron powder diffractometer at the NIST Center for Neutron Research. Synchrotron x-ray diffraction data was collected over the range of $0.5^\circ\text{--}38^\circ$ using the 11-BM High Resolution Powder Diffractometer at the Advanced Photon Source at Argonne National Laboratory. Crystal structures were refined using the Rietveld technique

^{a)}Author to whom correspondence should be addressed. Electronic mail: davies@seas.upenn.edu.

via the General Structure Analysis System (GSAS) using the EXPGUI graphical interface.^{14,15} Dielectric properties were investigated as a function of frequency and temperature using an impedance analyzer on pellets that were coated with a fired Ag paint Heraeus ST1601-14 type to provide electrical contacts for Pt leads.

III. RESULTS AND DISCUSSION

Compositions in the $(1-x)[(1-y)\text{PbTiO}_3-(y)\text{Bi}(\text{Zn}_{1/2}\text{Ti}_{1/2})\text{O}_3]-(x)\text{Bi}(\text{Mg}_{1/2}\text{Ti}_{1/2})\text{O}_3$ ternary system were synthesized at temperatures between 800 °C and 1100 °C. The locations of the compositions investigated within the ternary system are shown in Fig. 1. The compositions fall along one of two pseudo-binary solid-solution lines: $(1-x)[(0.9)\text{PbTiO}_3-(0.1)\text{Bi}(\text{Zn}_{1/2}\text{Ti}_{1/2})\text{O}_3]-(x)\text{Bi}(\text{Mg}_{1/2}\text{Ti}_{1/2})\text{O}_3$ [90/10] and $(1-x)[(0.75)\text{PbTiO}_3-(0.25)\text{Bi}(\text{Zn}_{1/2}\text{Ti}_{1/2})\text{O}_3]-(x)\text{Bi}(\text{Mg}_{1/2}\text{Ti}_{1/2})\text{O}_3$ [75/25]. These lines are differentiated by the concentration of BZT in the binary end-member ($y=0.1$ and 0.25 , respectively). These end-members have c/a ratios of 1.073 and 1.087, respectively, compared to 1.065 for PbTiO_3 and T_C of 535 °C and 590 °C compared to 490 °C for PbTiO_3 .

Neither of the Bi-based end-members are stable single-phase perovskites at ambient pressure; consequently, a large region of the ternary diagram near those end-members is multiphase. Single-phased compositions surrounding the PT end-member are tetragonal at room temperature. The c/a ratio of this structure increases with BZT substitution and decreases with BMT substitution. A morphotropic-type phase boundary exists in the single-phase region in the PT- and BMT-rich part of the diagram. The lattice parameters for the two investigated pseudo-binary solid solutions are shown in Fig. 2, which also includes data from the PT-BMT binary system.^{6,16,17}

Solid solutions of the [75/25] end-member could be formed with up to ~60% substitution of BMT. Typical of

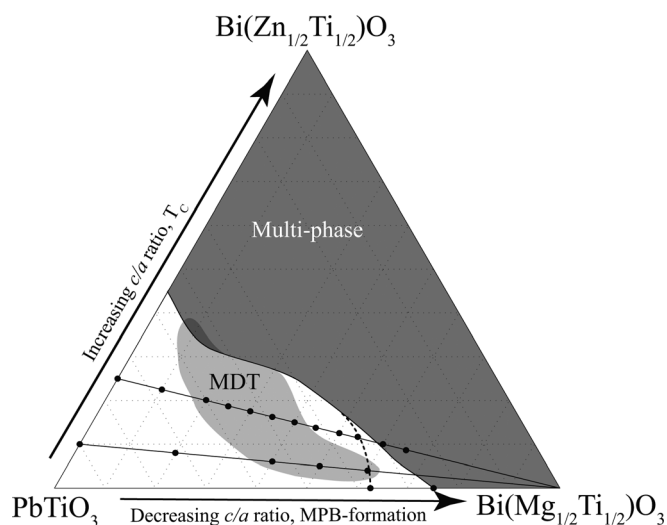


FIG. 1. Schematic phase diagram for the PT-BZT-BMT system. Compositions investigated along the $(1-x)[90/10]-(x)\text{BMT}$ and $(1-x)[75/25]-(x)\text{BMT}$ pseudo-binary lines are denoted by filled circles. The dashed line represents the approximate position of the morphotropic-type phase boundary. The light gray region denotes the region where multiple dielectric transitions (MDT) were observed.

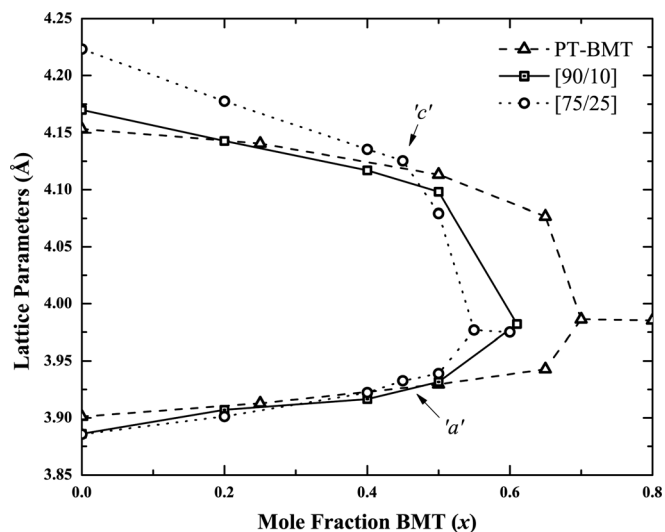


FIG. 2. Lattice parameters as a function of BMT substitution for the $(1-x)[90/10]-(x)\text{BMT}$ and $(1-x)[75/25]-(x)\text{BMT}$ solid solutions. Data from PT-BMT are also included.¹⁶ Convergence of the lattice parameters indicates the approximate position of MPB-type phase boundary.

Bi-containing compositions, small amounts of impurities are observed in the XRD patterns. The structure of the solid solution behaves as expected: From a starting c/a ratio of 1.087 at the [75/25] end-member the tetragonal distortion decreases with increasing BMT content until an MPB, as defined by the loss of tetragonality in the XRD pattern, is reached at $x=0.55$. The solid solution with the [90/10] end-member exhibits similar behavior, though diffraction patterns are free of peaks from impurity phases. Again the c/a of the PT-BZT end-member is reduced with increasing levels of BMT and an MPB is formed near a substitution of 60%. The lattice parameter data reveals that as the tetragonality of the PT-BZT end-member increases the concentration of the BMT additive required to induce the formation of an MPB is reduced. This result is somewhat surprising, as it might be expected that end-members with a higher c/a would require increasing concentrations of the MPB-forming additive (BMT) to reduce the tetragonality and form an MPB. These results suggest the opposite is true in these systems.

In all known MPB-forming systems the T_C at the MPB is lower than the T_C of the tetragonal end-member; we expected to observe the same trend in PT-BZT-BMT. However, as shown in Figs. 3 and 4 for the [90/10]-BMT and [75/25]-BMT solid solutions, respectively, no significant reduction in T_C , as measured by maximum permittivity, was observed over the range of the investigated compositions. At the MPB composition ($x=0.55$) the T_C for the [75/25]-BMT system is 585 °C, similar to the enhanced tetragonality PT-BZT end-member (590 °C). In the [90/10]-BMT system the T_C s actually show a small increase over the range of substitution. These transition temperatures are significantly higher than the MPB compositions in the PT-BiScO₃ (450 °C) and PT-BMT (425 °C) systems.^{6,7} The high T_C values in this ternary system suggest the presence of large, stable cation displacements, and possibly enhanced piezoelectric properties.

However, the permittivities of the ternary PT-BZT-BMT ceramics exhibit some unusual features. Usually

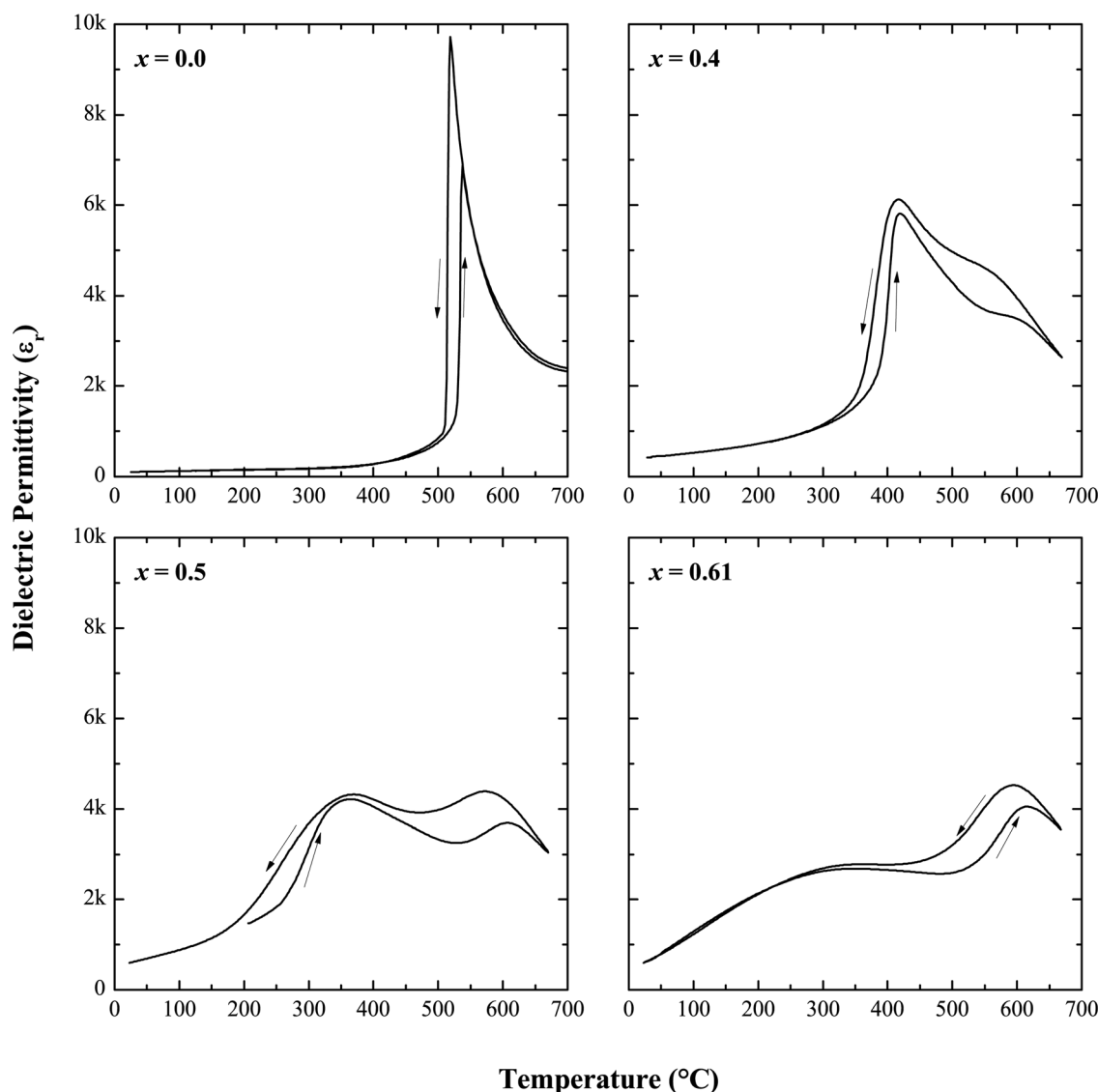


FIG. 3. Dielectric response ($f = 100$ kHz) for compositions in the $(1-x)[90/10]-(x)\text{BMT}$ solid solution. Arrows indicate the direction of thermal ramp.

tetragonal PT-based perovskite solid solutions exhibit a single dielectric maximum at the Curie temperature associated with the transition to a cubic paraelectric phase. This is not the case for many compositions in both the [90/10]-BMT and [75/25]-BMT solid solutions. Compositions with $x \geq 0.4$ in the $(1-x)[90/10]-(x)\text{BMT}$ solid solution and $0.2 \geq x \geq 0.35$ in the $(1-x)[75/25]-(x)\text{BMT}$ solid solution exhibit multiple dielectric transitions. In these compositions, one high-temperature transition is observed near 600°C while the other decreases in temperature as the BMT levels increase. Thermal hysteresis is observed in both sets of dielectric transitions, suggesting a structural origin necessitating a nucleation process.

The systematic variance of these dielectric transitions with BMT substitution is shown for the [75/25]-BMT solid solutions in Fig. 5. Along this pseudo-binary, the temperature of the higher transition remains nearly constant ($\sim 600^\circ\text{C}$) while the temperature of the lower transition decreases with increasing BMT levels. Beyond $x = 0.45$ only

the higher temperature maximum is observed. Similar behavior was observed along the [90/10]-BMT line, though a larger BMT concentration is required to induce the multiple transitions.¹⁶

The multiple dielectric transitions in the PT-BZT-BMT system are observed in a region characterized by a large occupancy of Bi cations on the A-site as well as a majority occupancy of FE-active cations ($\text{Ti}^{4+} + \text{Zn}^{2+}$) on the B-site; see Fig. 1. Consistent with this characterization, pseudo-binary solid solutions with higher BZT content exhibited the behavior at a lower concentration of BMT. There is also some evidence of this behavior in the $(1-x)\text{PT}-(x)\text{BMT}$ binary system ($x = 0.65$) published elsewhere.⁶

Maxima in the dielectric permittivity are usually associated with a structural transition. However, the compositions exhibiting multiple dielectric transition behavior in the PT-BZT-BMT system do not have an obvious structural explanation as the room-temperature structure is tetragonal and only one symmetry transition to the paraelectric cubic phase

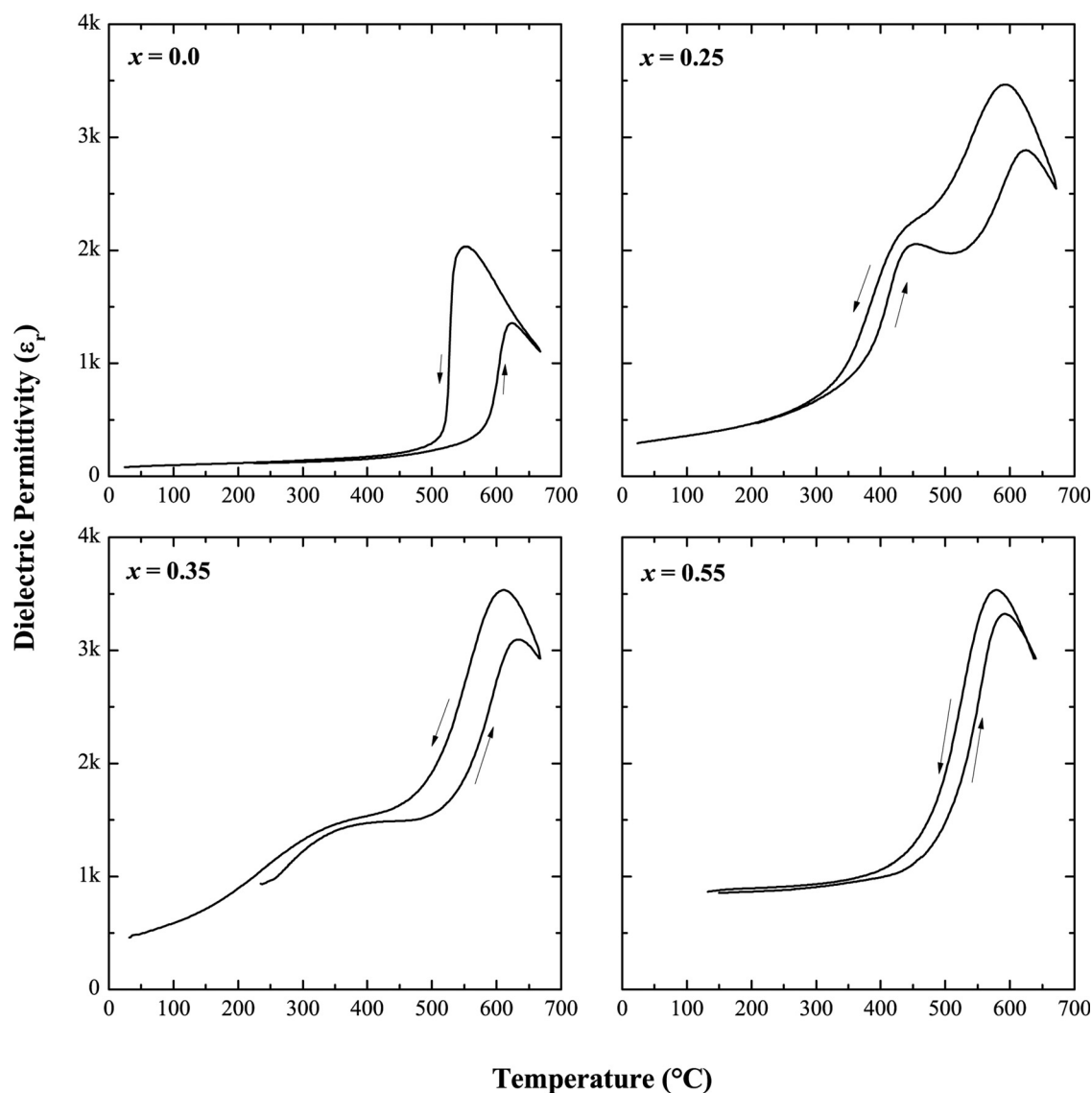


FIG. 4. Dielectric response ($f = 100$ kHz) for compositions in the $(1-x)[75/25]-(x)\text{BMT}$ solid solution. Arrows indicate the direction of thermal ramp.

is accessible. Still, the observation of thermal hysteresis in these compositions suggests that an unknown structural transition is occurring.

To investigate the structural response of this ternary system above room temperature, two compositions with well-spaced dielectric maxima and relatively large maximum permittivities were selected for temperature-dependent diffraction studies. The first composition, $(0.5)[90/10]-(0.5)\text{BMT}$, is tetragonal at room temperature with a c/a ratio of 1.054. The dielectric response for this composition is shown in Fig. 3. Dielectric permittivity maxima are located at $T = 385^\circ\text{C}$ and 590°C with a small hysteresis between heating and cooling cycles ($\Delta T = 40^\circ\text{C}$ for the higher temperature maxima). The structural behavior of this composition was studied by neutron powder diffraction from 25 – 900°C .¹⁶

The neutron diffraction patterns were modeled using Rietveld refinement techniques. Above the second maximum the diffraction data clearly show the structure is cubic ($\text{Pm}\bar{3}\text{m}$ -type). Below the first dielectric maximum, the scattering data can be refined with a P4mm lead titanate-type

tetragonal structure, though asymmetric peak broadening reduced the quality of the fit relative to the high temperature cubic phase ($\chi^2 = 1.998$ at 250°C versus $\chi^2 = 1.678$ at 800°C). The model is unable to properly account for observed intensity found between peaks in families split due to the tetragonal symmetry. This broadening is often observed in these highly tetragonal systems and complicates the fitting process, particularly in the intermediate temperature range, between the two dielectric maxima, where it contributes to peak overlap.⁵

Various models (space groups: P4mm , $\text{R}\bar{3}\text{c}$, $\text{R}\bar{3}\text{m}$, $\text{Pm}\bar{3}\text{m}$, and 2-phase combinations) were fit to the data in the intermediate temperature region; the best quality of fit was obtained for a single-phase structure with a small tetragonal distortion. The lattice parameters derived from these refinements are plotted in Fig. 6 as a function of temperature.¹⁶ With increasing temperature, the a and c lattice parameters converge (c/a decreases) up to the first dielectric transition. The structure then enters what appears to be a region of “persistent tetragonality” where the effect of temperature on the contraction of c is much weaker.

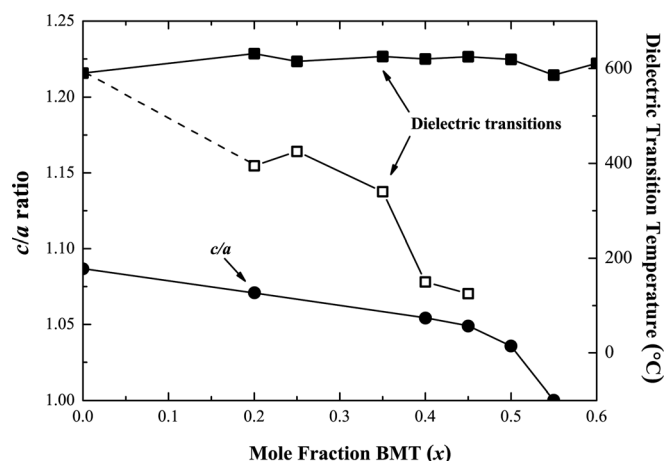


FIG. 5. c/a ratio and dielectric transition temperatures as a function of composition in the $(1-x)[75/25]-(x)\text{BMT}$ solid solution.

Beyond the higher temperature dielectric maxima the structure transforms to a well-fit cubic phase.

The structure of a second composition, $(0.75)[75/25]-(0.25)\text{BMT}$, was also investigated at high temperature, in this case using synchrotron x-rays rather than neutrons. This composition has a higher concentration of Zn^{2+} and lower concentration of Bi^{3+} relative to the $(0.5)[90/10]-(0.5)\text{BMT}$ composition. At room temperature the sample has a larger c/a ratio (1.070 versus 1.054) and dielectric transitions at 445 °C and 610 °C; see Fig. 4.

Rietveld refinement analysis of the synchrotron data revealed that at all temperatures the structure can be well modeled by a tetragonal ($P4mm$) and cubic ($Pm3m$) perovskite or a combination of the two.¹⁶ Temperature-dependent lattice parameters for $(0.75)[75/25]-(0.25)\text{BMT}$ are plotted in Fig. 7.¹⁶ A single-phase tetragonal structure is observed from room temperature up to 525 °C where peaks from a cubic modification are first resolved. The c/a of the tetragonal phase decreases with increasing temperature until it reaches 1.014 at 625 °C; at higher temperatures the structure is cubic. A region of two-phase tetragonal and cubic coexis-

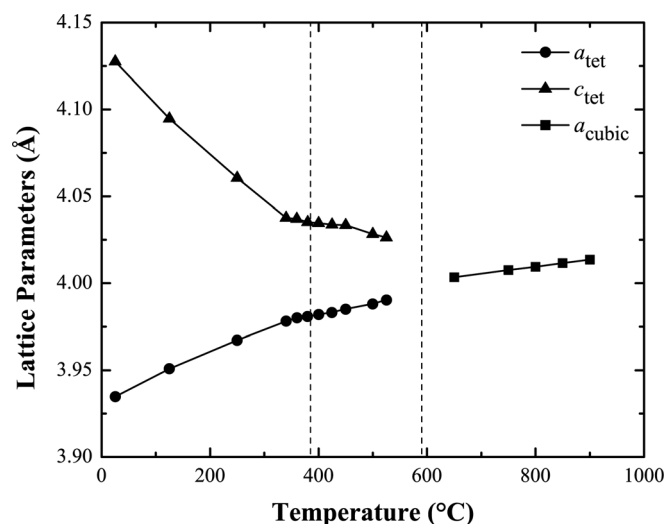


FIG. 6. Lattice parameters as a function of temperature for the $(0.5)[90/10]-(0.5)\text{BMT}$ composition. Vertical dashed lines represent the dielectric transition temperatures.

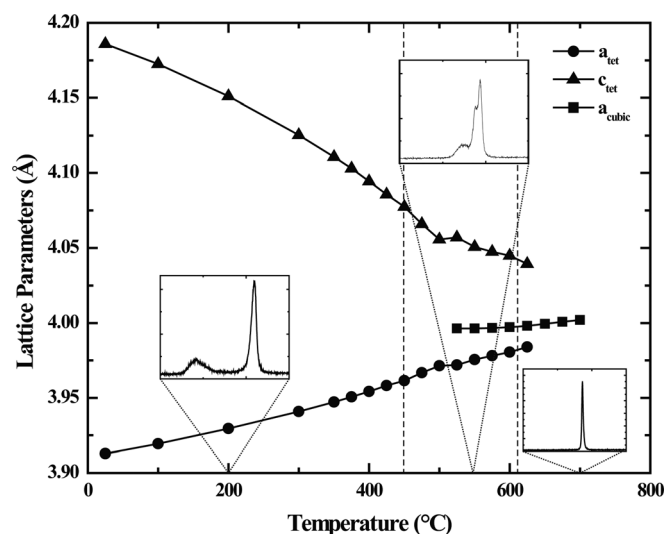


FIG. 7. Lattice parameters as a function of temperature for the $(0.75)[75/25]-(0.25)\text{BMT}$ composition. Insets plot the evolution of the $\{200\}$ family of peaks at representative temperatures.

tence is observed at a temperatures higher than the first dielectric maximum (525 °C versus 445 °C) and persists to a temperature that is slightly higher than the “averaged” second dielectric transition (625 °C versus 610 °C) but consistent with the thermal hysteresis of the dielectric response.

The two-phase coexistence in $(0.75)[75/25]-(0.25)\text{BMT}$ is superficially different to the “persistent tetragonality” observed in $(0.5)[90/10]-(0.5)\text{BMT}$. However, the asymmetric peak broadening in the tetragonal structure leaves open the possibility of an unresolvable cubic phase in the $(0.5)[90/10]-(0.5)\text{BMT}$ composition. An explicit 2-phase model applied to the neutron profiles showed no statistical improvement over a single tetragonal phase; however, it should be noted the resolution of the synchrotron data is greater than that of the data collected using neutrons. It is also possible that the differing macroscopic structural behavior is related to the Bi:Pb content; $(0.5)[90/10]-(0.5)\text{BMT}$ has a larger concentration of Bi^{3+} cations than $(0.75)[75/25]-(0.25)\text{BMT}$. For example, if the tetragonal regions at elevated temperatures are associated with Bi^{3+} -rich unit cells and the cubic phase with Pb^{2+} -rich regions, then the higher Bi concentration may be influencing the macroscopic symmetry observed by diffraction.

In both compositions investigated, the high temperature dielectric maximum is associated with a Curie-type transition from a ferroelectric tetragonal phase to a paraelectric cubic phase. If the structural behavior of these two compositions is consistent throughout the pseudo-binary solid solutions investigated, the PT-BZT-BMT ternary system exhibits MPB compositions with T_{CS} significantly higher (~ 150 °C) than previously reported systems.

IV. CONCLUSION

The ternary PT-BZT-BMT system was investigated in an attempt to capture the larger displacements of Bi^{3+} cations at an MPB and improve the transition temperature and piezoelectric properties while reducing the Pb-content. In a

region of phase space in the ternary system characterized by a large Bi^{3+} A-site occupancy (>40%) and high FE-active cation B-site occupancy (>75%) compositions that are tetragonal at room temperature exhibit two dielectric constant maxima above room temperature. Temperature-dependent diffraction studies revealed that a tetragonal symmetry persists in at least a portion of the crystal (depending on composition) to the high temperature dielectric transition.

ACKNOWLEDGMENTS

D.M.S. and P.K.D. were supported by the Office of Naval Research (ONR) through Grant No. N00014-09-1-0455. I.G. and A.M.R. were supported by the Office of Naval Research (ONR) under grant N00014-09-1-0157.

¹R. Cohen, *Nature* **358**, 136 (1992).

²P. Baettig, C. F. Schelle, R. LeSar, U. V. Waghmare, and N. A. Spaldin, *Chem. Mater.* **17**, 1376 (2005).

³A. A. Belik, S. Iikubo, K. Kodama, N. Igawa, S. Shamoto, S. Niitaka, M. Azuma, Y. Shimakawa, M. Takano, F. Izumi, and E. Takayama-Muromachi, *Chem. Mater.* **18**, 798 (2006).

⁴A. A. Belik, T. Wuernisha, T. Kamiyama, K. Mori, M. Maie, T. Nagai, Y. Matsui, and E. Takayama-Muromachi, *Chem. Mater.* **18**, 133 (2006).

⁵I. Grinberg, M. R. Suchomel, W. Dmowski, S. E. Mason, H. Wu, P. K. Davies, and A. M. Rappe, *Phys. Rev. Lett.* **98**, 107601 (2007).

⁶C. A. Randall, R. Eitel, B. Jones, T. R. Shrout, D. I. Woodward, and I. M. Reaney, *J. Appl. Phys.* **95**, 3633 (2004).

⁷R. E. Eitel, C. A. Randall, T. R. Shrout, P. W. Rehrig, W. Hackenburger, and S. E. Park, *Jpn. J. Appl. Phys.* **40**, 5999 (2001).

⁸I. Grinberg, I. M. R. Suchomel, P. K. Davies, and A. M. Rappe, *J. Appl. Phys.* **98**, 094111 (2005).

⁹I. Grinberg and A. M. Rappe, *Phys. Rev. Lett.* **98**, 037603 (2007).

¹⁰M. R. Suchomel and P. K. Davies, *Appl. Phys. Lett.* **86**, 262905 (2005).

¹¹D. M. Stein, M. R. Suchomel, and P. K. Davies, *Appl. Phys. Lett.* **89**, 132907 (2006).

¹²S. A. Fedulov, *Sov. Phys. Solid State* **6**, 375 (1964).

¹³S. Nomura, K. Kaneta, J. Kuwata, and K. Uchino, *Mater. Res. Bull.* **17**, 1471 (1982).

¹⁴A. C. Larson and R. B. Von Dreele, "General Structure Analysis System (GSAS)," Los Alamos National Laboratory Report LAUR 86-748 (2000).

¹⁵B. H. Toby, *J. Appl. Cryst.* **34**, 210 (2001).

¹⁶See supplementary material at <http://dx.doi.org/10.1063/1.3646559> for relevant diffraction patterns, c/a ratio and dielectric transition temperatures as a function of composition in the $(1-x)[90/10]-(x)\text{BMT}$ solid solution, and structural parameters and reliability statistics from Rietveld analyses.

¹⁷M. R. Suchomel and P. K. Davies, *J. Appl. Phys.* **96**, 4405 (2004).